

REPORT DOCUMENTATION PAGE

Form Approved
OMB No. 0704-0188

Public reporting burden for this collection of information is estimated to average 1 hour per response, including the time for reviewing instructions, searching existing data sources, gathering and maintaining the data needed, and completing and reviewing the collection of information. Send comments regarding this burden estimate or any other aspect of this collection of information, including suggestions for reducing this burden, to Washington Headquarters Services, Directorate for Information Operations and Reports, 1215 Jefferson Davis Highway, Suite 1204, Arlington, VA 22202-4302, and to the Office of Management and Budget, Paperwork Reduction Project (0704-0188), Washington, DC 20503.

1. AGENCY USE ONLY (Leave Blank)	2. REPORT DATE <i>March 1999</i>	3. REPORT TYPE AND DATES COVERED <i>Technical</i>	
4. TITLE AND SUBTITLE Wave Propagation Model and Simulations for Landmine Detection		5. FUNDING NUMBERS <i>DAAG55-98-1-0401</i>	
6. AUTHORS Ammar Y. Rathore Thomas P. Weldon			
7. PERFORMING ORGANIZATION NAME(S) AND ADDRESS(ES) Department of Electrical Engineering University of North Carolina at Charlotte 9201 University City Boulevard Charlotte, NC 28223		8. PERFORMING ORGANIZATION REPORT NUMBER	
9. SPONSORING / MONITORING AGENCY NAME(S) AND ADDRESS(ES) U.S. Army Research Office P.O. Box 12211 Research Triangle Park, NC 27709-2211		10. SPONSORING / MONITORING AGENCY REPORT NUMBER <i>ARO 38897.2-MA-LMD</i>	
11. SUPPLEMENTARY NOTES The views, opinions and/or findings contained in this report are those of the author(s) and should not be construed as an official Department of the Army position, policy or decision, unless so designated by other documentation.			
12a. DISTRIBUTION / AVAILABILITY STATEMENT Approved for public release; distribution unlimited.		12b. DISTRIBUTION CODE	
13. ABSTRACT (<i>Maximum 200 words</i>) A simplified 1-dimensional transmission light model of electromagnetic waves propagation in mine fields is considered. This model might be used as a first indicator of the presence of land mines. Next, the 2D inverse algorithm would image mines. It is shown that this 1-dimensional model is in general agreement with published Army data.			
14. SUBJECT TERMS transmission line model, attenuation of GPR signal, air-gaps, TNT		15. NUMBER OF PAGES 18	16. PRICE CODE
17. SECURITY CLASSIFICATION OF REPORT UNCLASSIFIED	18. SECURITY CLASSIFICATION OF THIS PAGE UNCLASSIFIED	19. SECURITY CLASSIFICATION OF ABSTRACT UNCLASSIFIED	20. LIMITATION OF ABSTRACT UL

Wave Propagation Model and Simulations for Landmine Detection (technical report)

Ammar Y. Rathore and Thomas P. Weldon

Department of Electrical Engineering
University of North Carolina-Charlotte
Charlotte, NC 28223

1. Introduction

Recently there has been interest in developing new equipment and models for the detection and removal of landmines from field using Ground Penetrating Radar. In this project landmines with and without air gap are modeled using conventional electrical simulation tools. Our approach is to use the time and frequency domain behaviors to support the development of equations for newly developed inverse mathematical solutions. The equations for the voltage in the transmission line models of this paper are identical to Maxwell's equations in one dimension for the Ground Penetrating Radar problem. Therefore, the results of this paper for solutions to the transmission line voltage are equivalent to the predicted E field for this problem. The transmission lines model plane waves propagation in the media of interest, also these lines are used since we already have a software to work for these lines. So, it is a matter of convenience.

An electromagnetic (EM) wave propagated from a GPR sees different media of different electrical properties. In Fig. 1, the transmitted electromagnetic wave propagates through different intervening layers of air, soil, and landmine materials. An air gap is taken into account before TNT because mines often contain 10-30% air. The uniform plane wave in Fig. 1 is governed by equations identical to transmission line equations. Thus, a transmission line model can be described that models the scenario in Fig. 1.

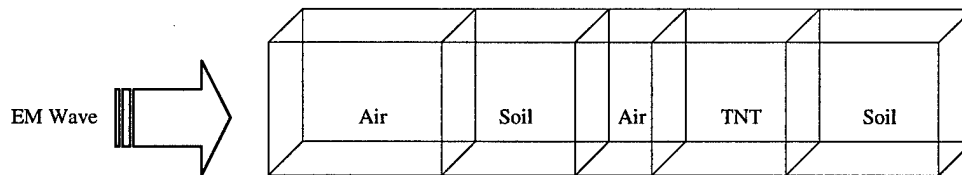


Figure 1. Multi layer Transmission model seen by transmitted EM wave.

When a travelling EM wave propagates through one medium and enters another with different electrical parameters, it experiences reflection. At all interfaces between different materials, part of the wave reflects back and the remainder moves forward. Each reflected component will be subjected additional reflections at material interfaces as it travels back toward the source (radar).

In the case of a pulsed EM source, the reflections will consist of time delayed pulses with strengths proportional to the strengths of the reflections. The pulse of interest is the one that reflects back from the landmine. Its final magnitude will be the product of initial pulse magnitude with the transmission and reflection coefficients of each intervening material. Also, the pulses are attenuated depending on the attenuation constant and length of each material. In section 2, we describe the relationship between the Electromagnetic wave models and transmission line models. In section 3 we provide results of the transmission line simulations.

2. Modeling Equations

19990706 074

First, let us consider the equations that define wave motion in lossy dielectrics. If a wave propagates in the +z direction, the x component of E field is given by [1]:

$$E_{xs} = E_{x0} e^{-\alpha z} e^{-j\beta z} \quad (1)$$

Where α and β are attenuation and phase constants respectively. These constants when combined give us propagation constant (γ) which is a complex quantity:

$$\gamma = \alpha + j\beta \quad (2)$$

In a lossy dielectric having permittivity ϵ , conductivity σ and permeability μ , propagation constant is given by:

$$\gamma = \pm \sqrt{j\omega\mu(\sigma + j\omega\epsilon)} \quad (3)$$

Where μ is magnetic permeability in Henry/m, σ is conductivity of the material in Siemens/meter, ω is frequency in radians/m, and ϵ in Farads/m.

The complex intrinsic impedance η of the medium (lossy dielectric) is given by:

$$\eta = \frac{E_{xs}}{H_{xs}} = \sqrt{\frac{j\omega\mu}{\sigma + j\omega\epsilon}} \quad (4)$$

For a dielectric material, the loss tangent δ is defined as:

$$\tan \delta = \frac{\sigma}{\omega\epsilon} \quad (5)$$

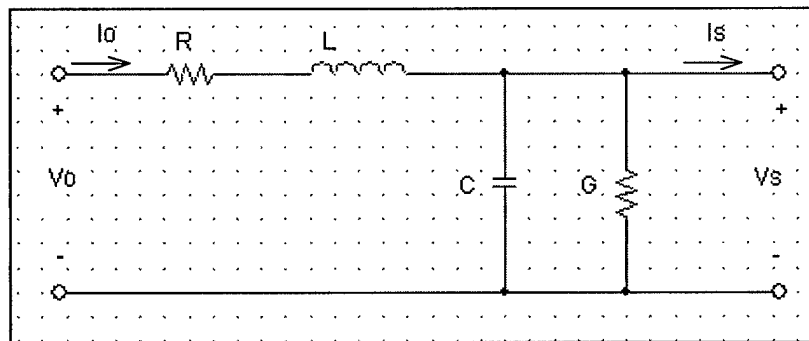


Figure 2. Equivalent circuit for section of a transmission line.

An equivalent circuit for section of a transmission line is shown in figure 2. For each equation listed above there is a similar transmission line equation. For example, voltage wave equation for the transmission line is given by:

$$V_s = V_0 e^{-\gamma z} \quad (6)$$

The propagation constant for the transmission line is

$$\gamma = \sqrt{(R + j\omega L)(G + j\omega C)}$$

Where R is resistance per unit length in Ohm/m, L is inductance per unit length in Henry/m, G is conductance per unit length in Siemens/m, and C is capacitance per unit length in Farads/m.

Finally, the characteristic impedance of a transmission line is defined as:

$$Z_0 = \frac{V_s}{I_s} = \sqrt{\frac{R + j\omega L}{G + j\omega C}} \quad (8)$$

On comparing equations 1 and 6 for both the cases, we find that they are identical. So the terms E and V can be used interchangeably (as can the terms H and I). By comparing equation pairs 1, 6; 3, 7; and 4, 8; it is clear that if in a transmission line we let $V = E$, $I = H$, $R = 0$, $L = \mu$, $G = \sigma$ and $C = \epsilon$, and $\eta = Z_0$, then the transmission line model is identical to the uniform plane wave propagation model.

The values of electrical properties [2] used for simulations are given in Table 1, using the constants $\mu_0 = 4\pi \times 10^{-7}$ H/m, $\mu_r = 1$, $R = 0$, $\epsilon_0 = 8.85 \times 10^{-12}$ F/m, $f = 1$ GHz.

Table 1: Electrical Properties & calculated parameters

	ϵ_r	α nepers/m	β radian/m	$\tan\delta$	$ Z_0 = \eta $ ohms	$\angle Z_0$ Degrees	$G = \sigma$ Siemens	$L = \mu$ micro henry	$C = \epsilon_0\epsilon_r$ Pico Farads
Air	1	0	20.98	0	376.6	0	0	1.26	8.85
Dry Soil	2.5	.417	33.17	.025	238.6	.72	.0035	1.26	22.12
Wet Soil 13% moisture	10	16.23	68.27	0.5	112.82	13.38	.28	1.26	88.4
TNT	2.86	.0319	35.48	.0018	223.14	.052	.286m	1.26	25.3

For one meter propagation distance, the amplitude of the transmitted pulse in dry soil falls $e^{-(.417)} = 0.659$ or $20\log(.659) = 3.62$ dB below its value at $z = 0$. For wet soil, the amplitude falls $e^{-(16.32)} = 8.94 \times 10^{-8}$ or nearly 141 dB below its value at $z = 0$.

3. Simulation Results

We did simulations using transmission line models in the Pspice 8.0 software package. A 1ns sinusoidal current pulse was applied at the input with a shunt resistance. Shunt resistance is used in some simulations to eliminate reflections of waves that propagate back to the source. For example, if a wave is reflected back from the termination and travels to the source end, it would be reflected again if source does not offer proper termination. Therefore a current pulse with a shunt resistor are used at the source end of transmission line model.

In the first experiment, the transmission-line model of air is simulated to verify that the impedance is the expected value $Z_0 = \eta = 377$ for air. The circuit used for simulation is shown in figure 3(a), where air transmission line has a length of 3 m and is properly terminated with a matched resistance of 377.3 Ω . The analogous physical situation is depicted in Fig. 3(b), where the reflector indicates that the source impedance is mismatched and the absorber indicates that the opposite end of the line is properly terminated (no reflections). As the EM wave propagates through the transmission line (modeling air) and reaches the termination resistor R, it is not reflected since the load end is matched with the 377 ohm transmission line.

The results of the simulation of the voltage at the antenna for an incident pulse are shown in Fig. 3(c). The antenna voltage (EM source in Fig. 1) is equivalent to the voltage at the junction of R5 and the transmission line in Fig. 3(a). The incident pulse is a 1 nanosecond wide 1 GHz sinusoidal pulse at time 1 ns. In Fig. 3(c), only the incident pulse is visible at time $t = 1\text{ ns}$ with no reflected pulses observed, confirming that the line impedance is 377 ohms. Finally, Fig. 3(d) shows the voltage at the antenna as the input frequency is swept from 1 GHz to 2 GHz. The frequency response varies from 375.88 to 375.93 Volts for a one ampere input, indicating that line impedance varies little from the desired 377 ohm impedance.

Figure 4(a) models the scenario of Fig. 4(b) consisting of 3 meters of air improperly terminated at both ends. This experiment is primarily used to confirm the velocity along the transmission line modeling air. As seen in Fig. 4(c), the reflection at approximately 20 ns after the incident pulse corresponds to the predicted round-trip time of the pulse through a 6 meter round-trip distance. The velocity closely approximates the speed of light of 0.3 meters per nanosecond. Fig. 4(d) shows the extreme impedance variations with respect to frequency, corresponding to perfect constructive or destructive interference.

In the experiment of Fig. 5, the transmission line of dry soil is used to investigate the impedance $Z_0 = \eta$ and propagation velocity in dry soil. The circuit used for simulation is shown in Fig. 5(a), where transmission line has a length of 3 m and is terminated with a resistance of 100000 Ω . This models the situation in Fig. 5(b) where the EM wave propagates through a highly reflective interface (mismatched), through dry soil, and reaches another highly reflective interface. Simulation for a pulsed sinusoid are given in Fig. 5(c). The incident pulse reaches a peak voltage of 238.91 volts indicating an impedance $Z_0 = \eta = 238.91$ ohms for dry soil. This corresponds to the predicted impedance of 238.6 in table 1, verifying our transmission line model. The amplitude of next pulse (36.49 V) corresponds to predicted attenuation of 3.62 dB/m. The time delay of 31 ns corresponds to a velocity of 0.19 meters per nanosecond or 0.65 c. This speed corresponds well with the speed predicted from the dielectric constant of table 1 for dry soil, 0.63 c. Finally, the frequency response in Fig. 5(d) shows that impedance varies from 202 ohms to 280 ohms as a function of the frequency of the source.

The experiment of Fig. 6 is used to investigate the impedance $Z_0 = \eta$ in wet soil. The circuit used for simulation is shown in Fig. 6(a), where transmission line has a length of 0.1 m and is terminated with a resistance of 100000 Ω . A shorter line length was necessary due to the high attenuation of wet soil. As EM wave propagates through the transmission line and reaches the termination resistor R, it is reflected. In Fig. 6(c), the incident pulse is shown at 1ns with a peak amplitude of 118.3V. Again this corresponds to the predicted impedance of $Z_0 = \eta = 112.8$ ohms in table 1. In middle plot reflected pulse is seen at 3ns. Finally, Fig 6(d) shows impedance variations with respect to frequency.

Next, a series of experiments are done on a combination of transmission lines modeling several possible scenarios derived from the scenario in Fig. 1. For these experiments, the source impedance (R5) is set equal to air impedance (377 ohm) to model a properly matched source antenna. The terminating impedance is taken to be a long length of wet or dry soil (effectively acting as an absorber due to attenuation).

The first experiment is shown in Fig. 7, where the reflection from an air gap in dry soil is investigated (in essence, a mine without TNT). The time-domain results are shown in Fig. 7(c), and frequency response in Fig. 7(d). As expected, the EM wave experiences large reflections at the air gap. The first reflection of 43.13V at 21ns represents the first air soil interface. The second reflection of 12.5V at 23.6ns is the mine air gap (second air gap) reflection. Since the 1cm gap is narrow, two reflections are not observed. This leads to a somewhat unusual shape for this second reflection. The lower portion of Fig. 7(c) shows the same response on a greatly expanded scale to make smaller secondary reflections visible.

In the experiment of Fig. 8, the reflection from an air gap in wet soil is investigated. Due to the large attenuation in wet soil, the depth of the wet soil before the air gap is only 10 cm. The time-domain results are shown in Fig. 8(c), and frequency response in Fig. 8(d). The first reflection of 113.4V at 21ns represents the first air soil interface, the second reflection of -295.4mV at 23.6ns is the mine air gap

reflection. The wet soil pulse (2nd pulse) is nearly obscured by the first pulse. The results are difficult to interpret, since this may be due in part to simulation parameters in the software package set-up.

The experiment of Fig. 9 is used to investigate the reflection from TNT in dry soil (in essence, a mine without any air gap). The time-domain results are shown in Fig. 9(c), and frequency response in Fig. 9(d). The incident pulse is seen in Fig 9(c) at 1 ns with a peak amplitude of 188V. The reflection of 43.35V at 21ns represents the first air soil interface, then reflection at 23.6ns is from the TNT. As compared to pulse width, the 10cm length of TNT is narrow. Therefore, we again see an unusual reflected pulse shape.

The experiment of Fig. 10 simulates a landmine buried in dry soil with an air gap. The time-domain results are shown in Fig. 10(c), and frequency response in Fig. 10(d). In Fig. 10(c), the incident pulse is seen at 1 ns with a peak amplitude of 188.15V. The reflection of 43.13V at 21ns represents the first air soil interface, then reflection at 23.6ns is from the second air/soil interface and TNT comprising the mine. The large envelope variations in Fig. 10(d) are induced by the presence of the mine.

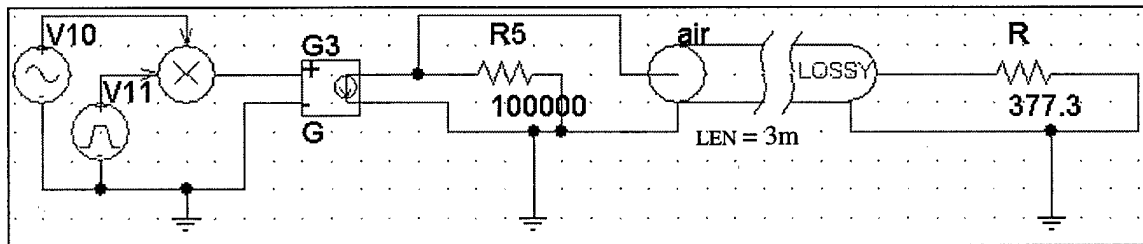


Figure 3(a). Transmission line model of air with improper source termination and matched load termination. Used to verify transmission line model parameters.

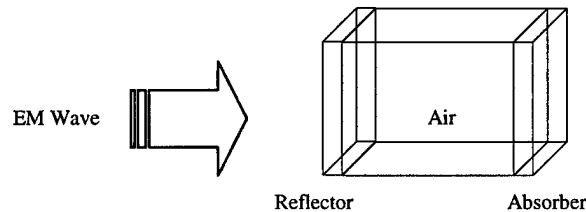


Figure 3(b). Analogy of circuit in Fig. 3(a).

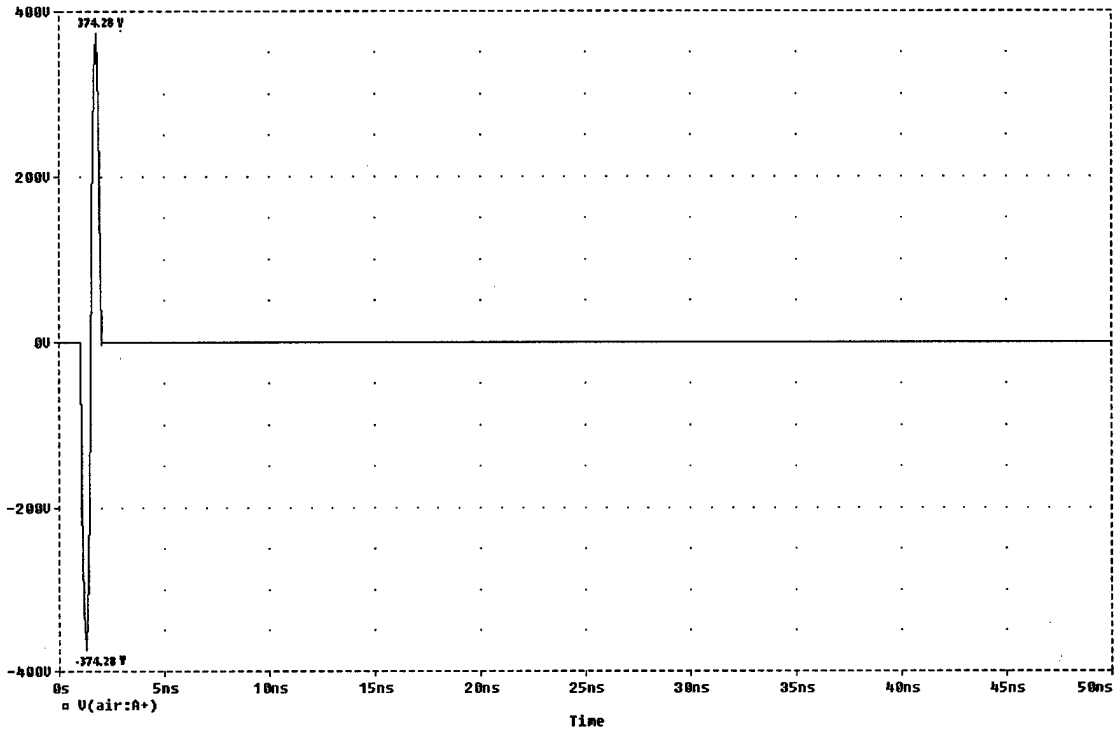


Figure 3(c). Voltage at the antenna (R5 in Fig. 3(a)), for circuit of Fig. 3(a). No reflections are observed since the line is properly terminated with a 377 ohm load.

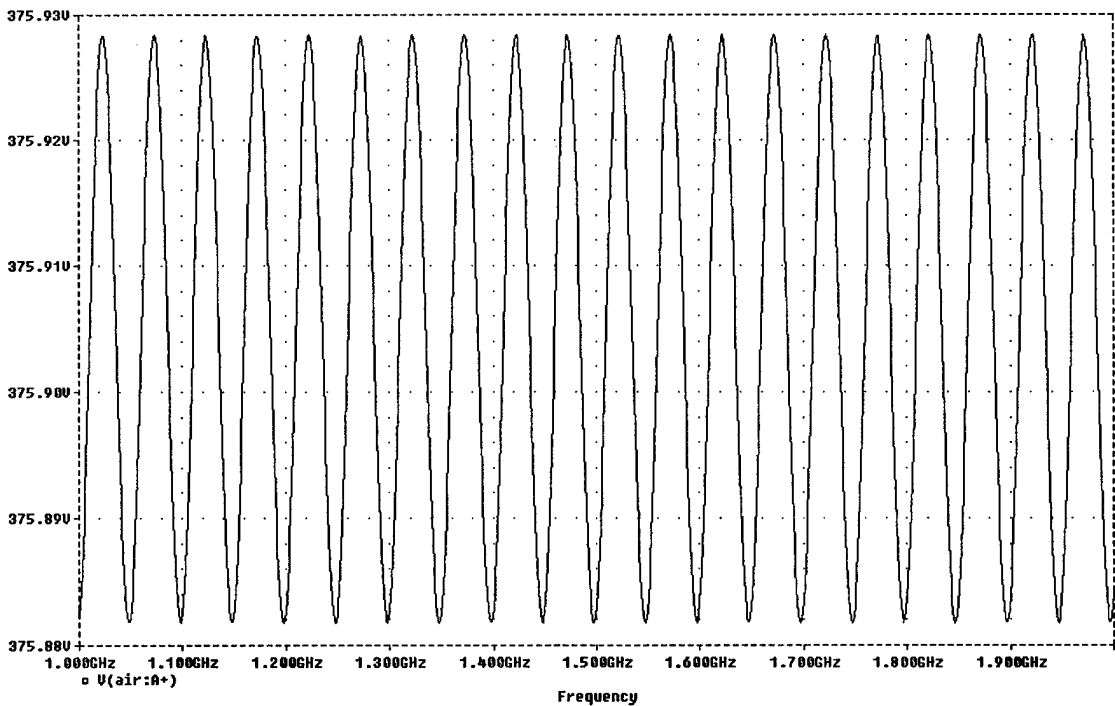


Figure 3(d). Voltage at the antenna (R5 in Fig. 3(a)), frequency sweep plot from 1 GHz to 2 GHz.

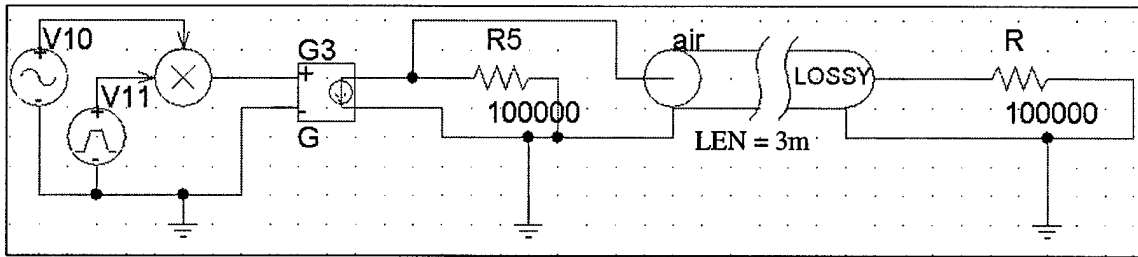


Figure 4(a). Transmission line model of air, terminated with 100KΩ. Used to measure velocity of pulse in transmission line.

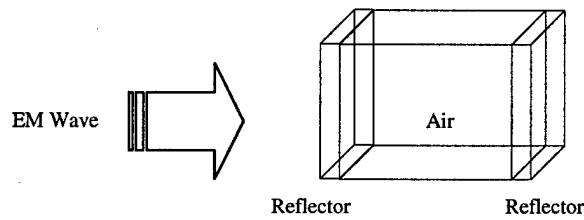


Figure 4(b): Analogy of circuit in Fig. 4(a).

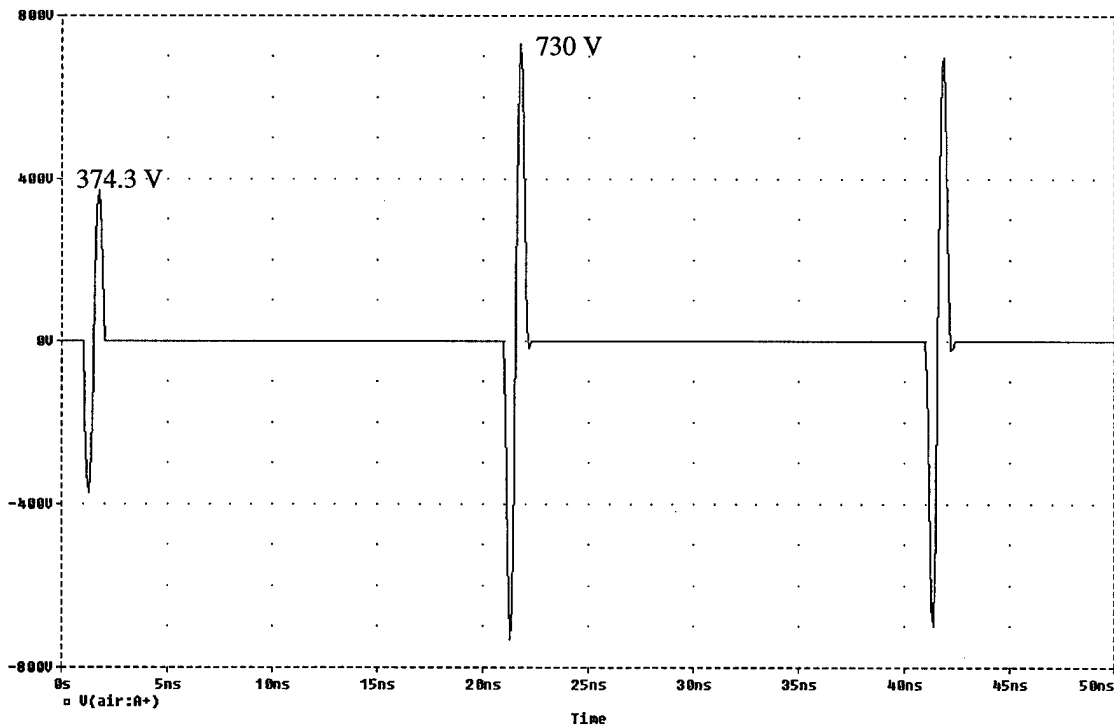


Figure 4(c). Voltage at the antenna (R5 in Fig. 4(a)), for 100K termination.

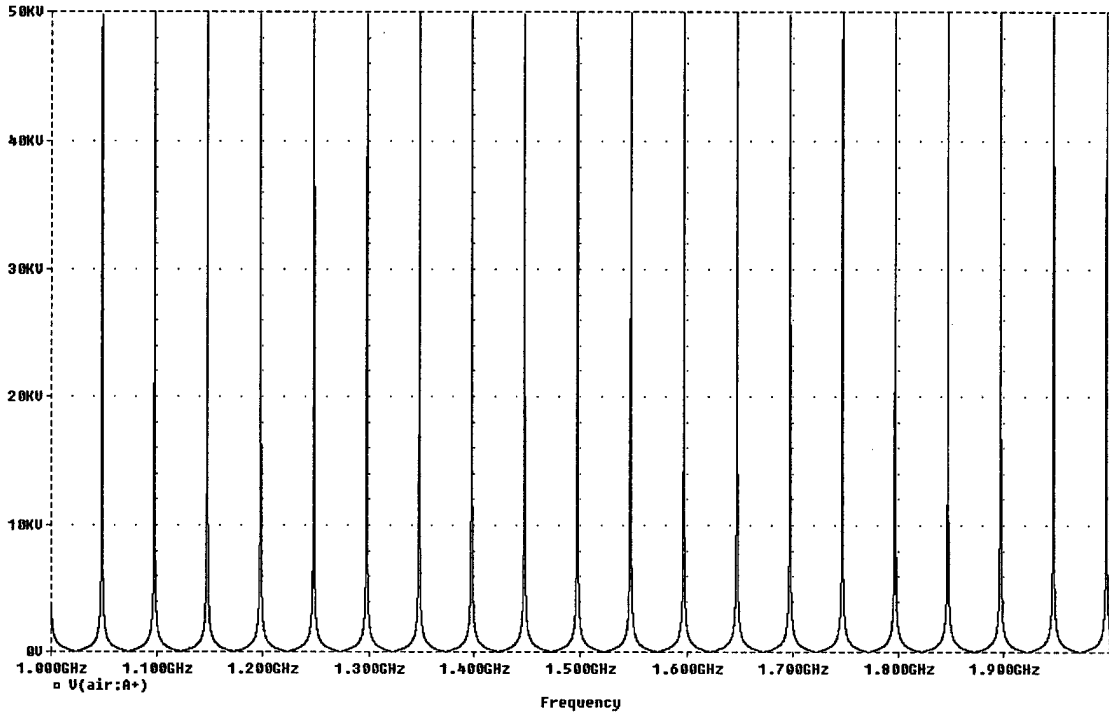


Figure 4(d). Voltage at the antenna (R5 in Fig. 4(a)), Frequency Sweep plot from 1GHz to 2GHz

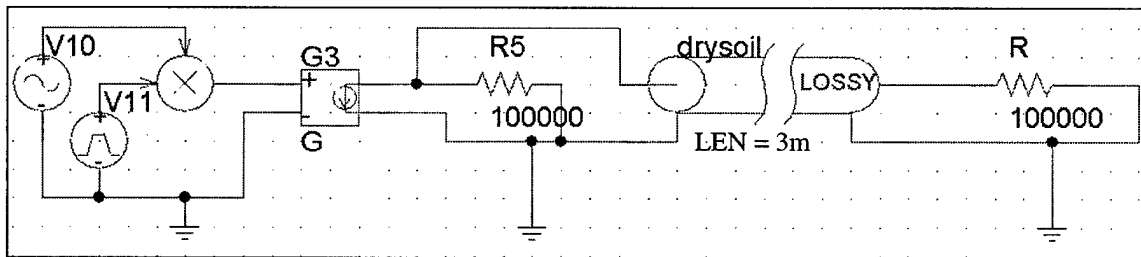


Figure 5(a). Transmission line model of dry soil. Used to check dry soil impedance and velocity

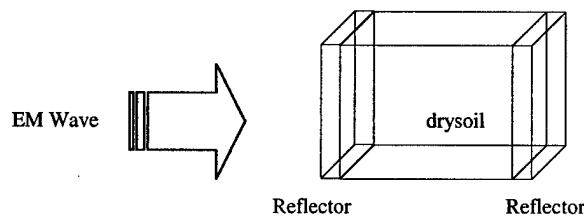


Figure 5(b). Analogy of circuit in Fig. 5(a).

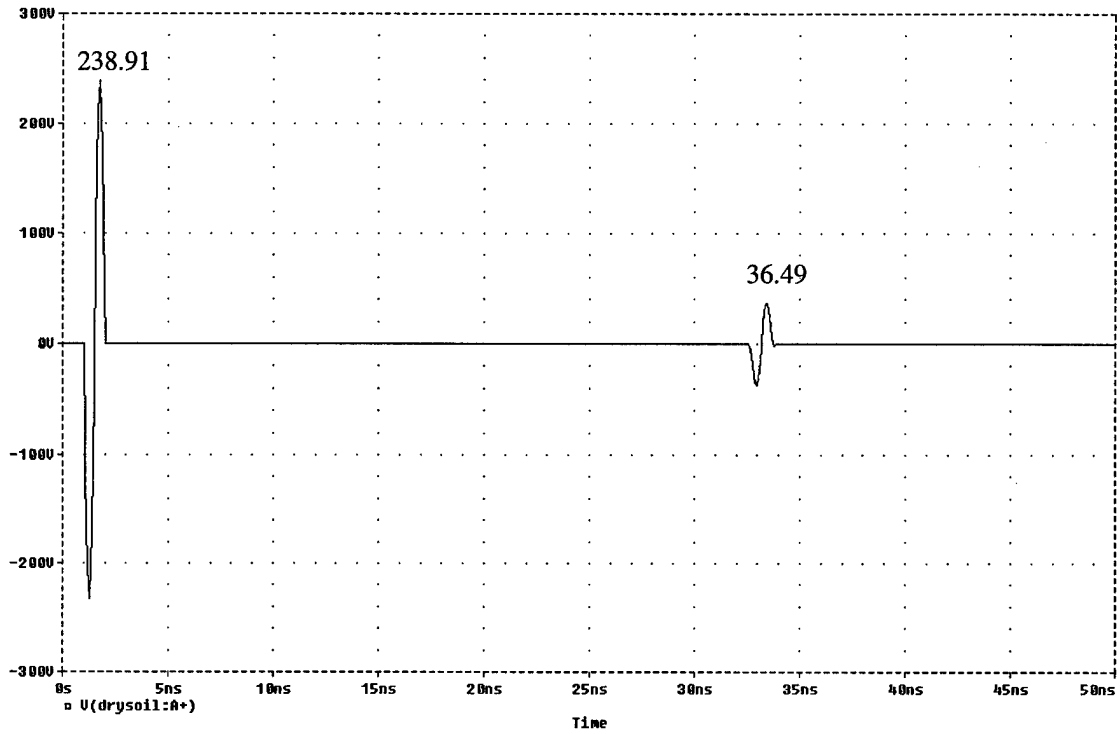


Figure 5(c). Voltage at the antenna (R5 in Fig. 5(a)), for Dry-Soil Model.

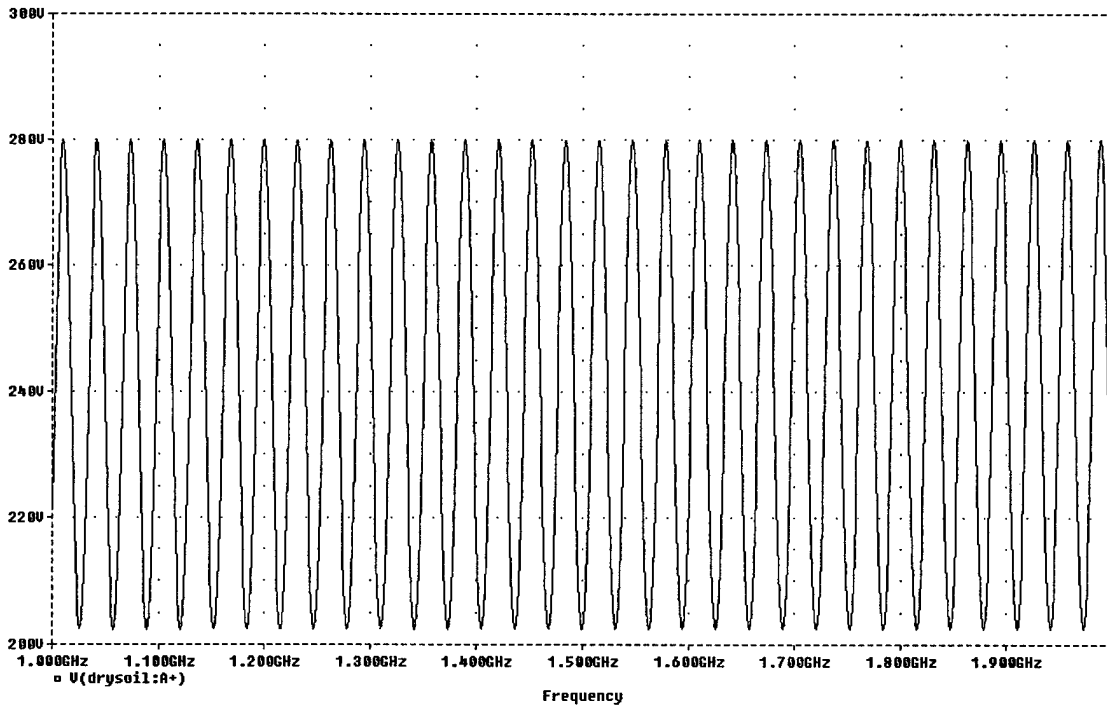


Figure 5(d). Voltage at the antenna for dry soil (R5 in Fig. 5(a)), Frequency Sweep plot from 1GHz to 2GHz

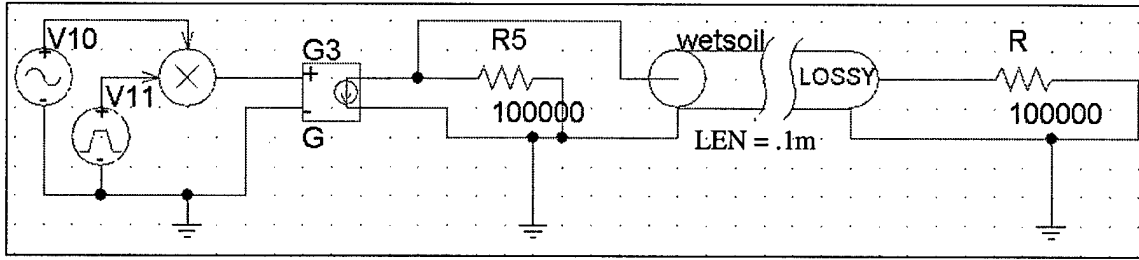


Figure 6(a). Transmission line model of wet soil. Used to check wet soil impedance

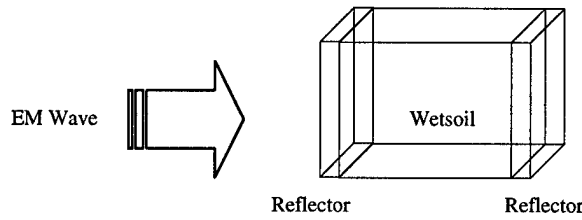


Figure 6(b): Analogy of circuit in Fig. 6(a).

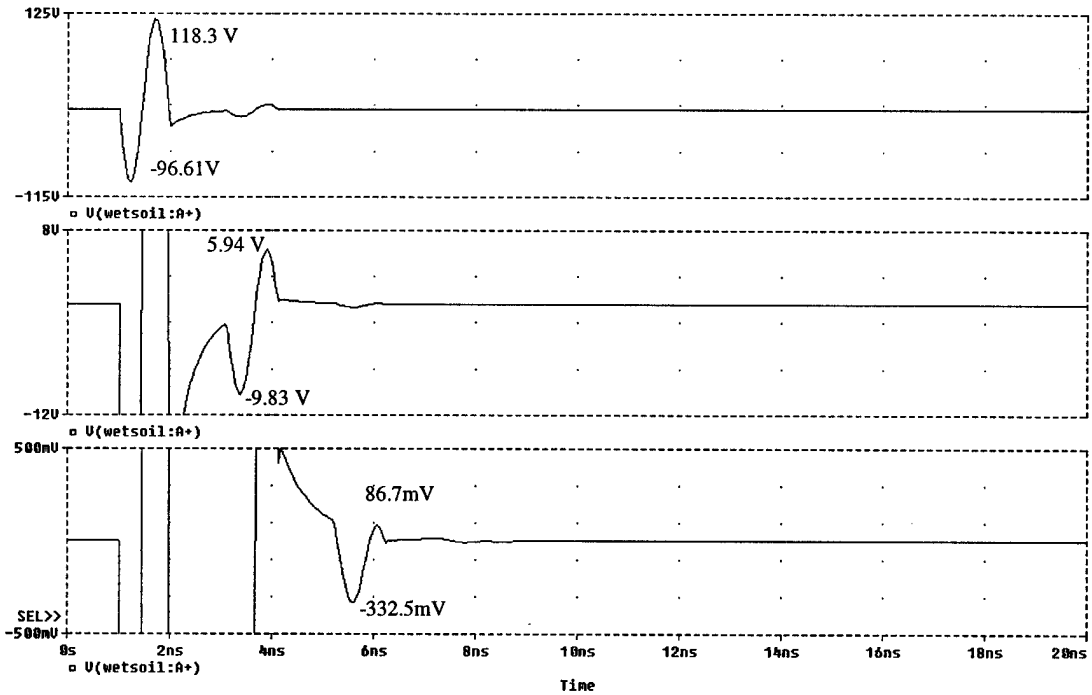


Figure 6(c). Voltage at the antenna for Wet-Soil Model with transmission line length = 0.1m. Top: Incident pulse occurs at 1ns; Middle: 0.2m round trip reflection pulse occurs at 3ns Bottom: 2nd reflection at 5ns.

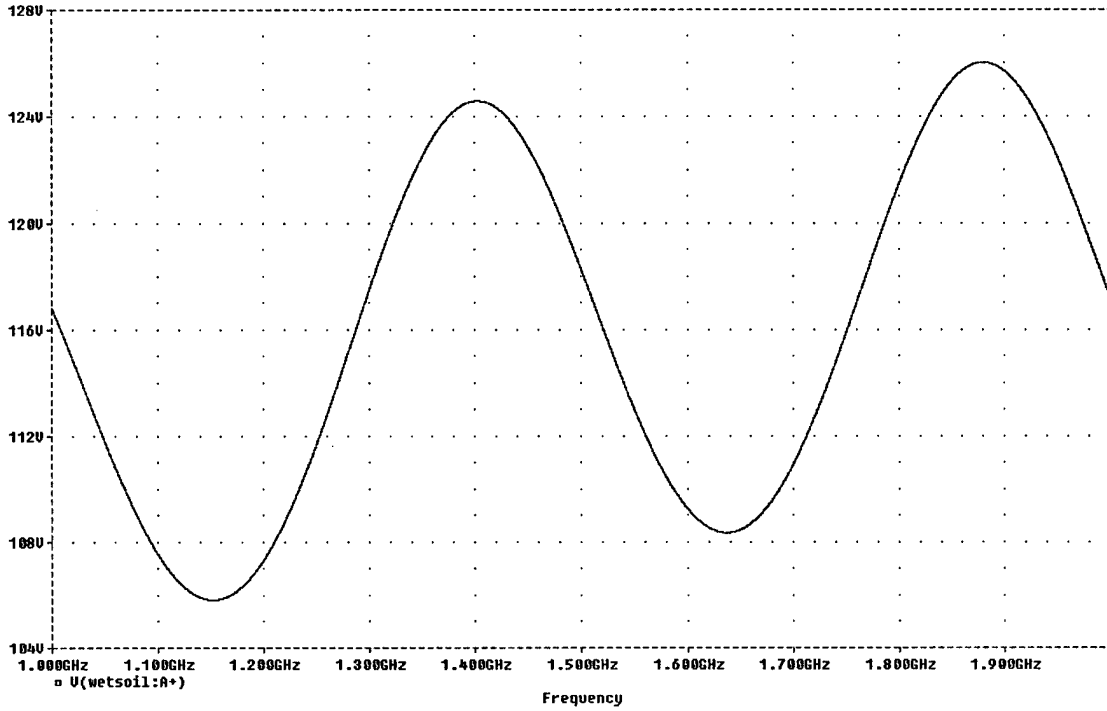


Figure 6(d). Voltage at the antenna (R5 in Fig. 6(a)) for Wet-Soil Model, Frequency Sweep plot from 1GHz to 2GHz

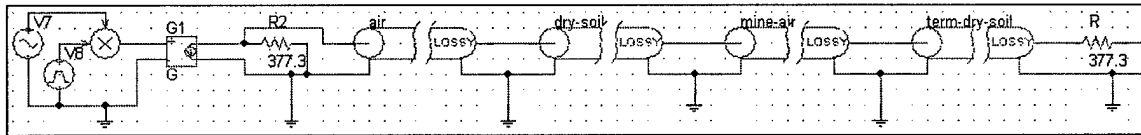


Figure 7(a). Air-drysoil-air-drysoil model. With lengths: air = 3m, drysoil = 0.25m, airgap = 1cm, and drysoil = 100m.

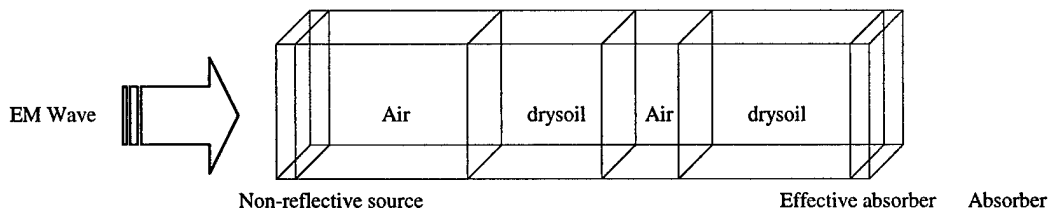


Figure 7(b). Analogy of circuit in Fig. 7(a).

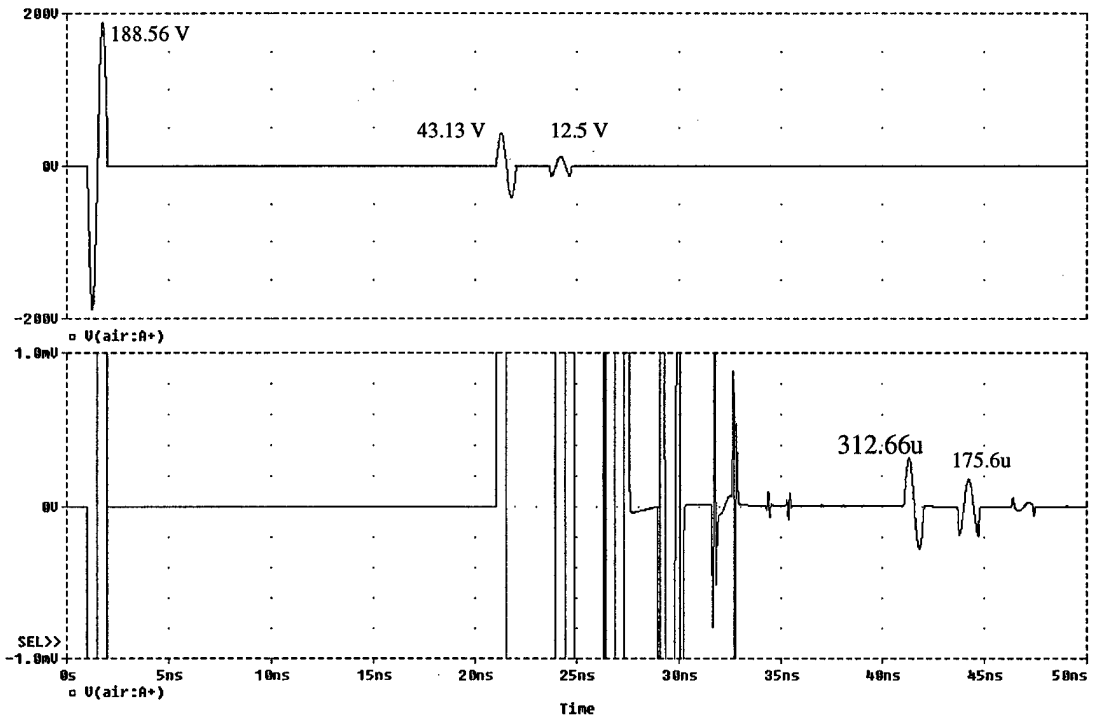


Figure 7(c). Voltage at the antenna (R5 in Fig. 7(a)) for Air-drysoil-air-drysoil model. With lengths: air = 3m, drysoil = 0.25m, airgap = 1cm and drysoil = 100m. Top: Normal view. First reflection occurs at 21ns. Bottom: Magnified view.

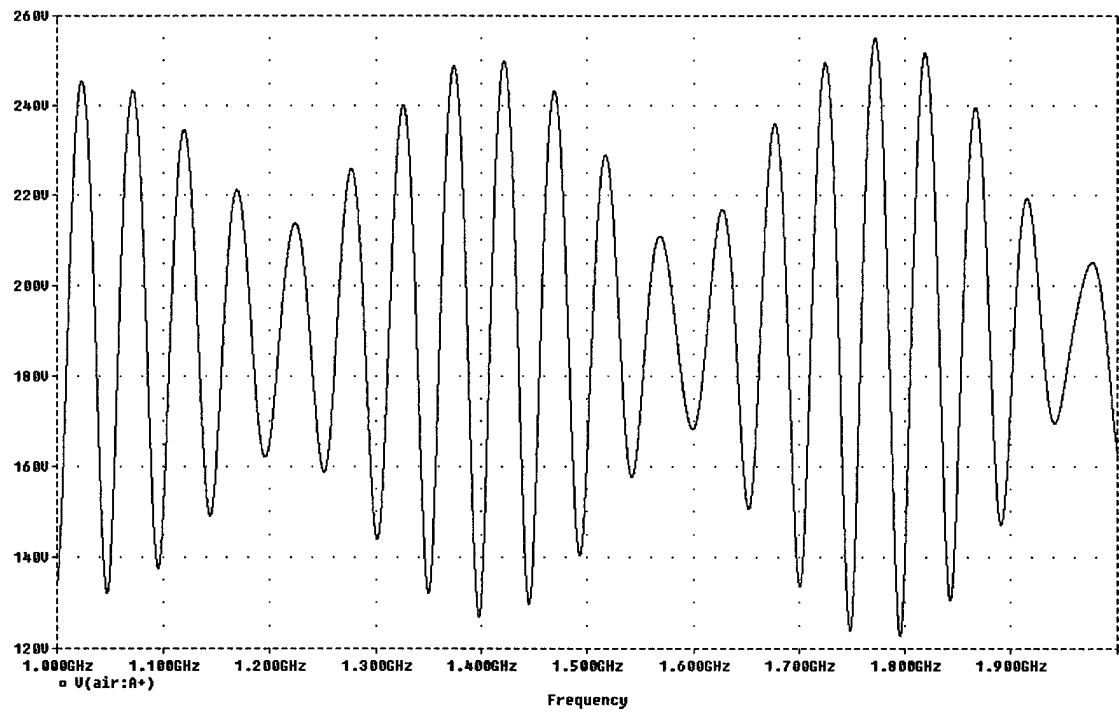


Figure 7(d). Voltage at the antenna (R5 in Fig. 7(a)) for Air-drysoil-air-drysoil model. With lengths: air = 3m, drysoil = 0.25m, airgap = 1cm and drysoil = 100m. Frequency Sweep plot from 1GHz to 2GHz

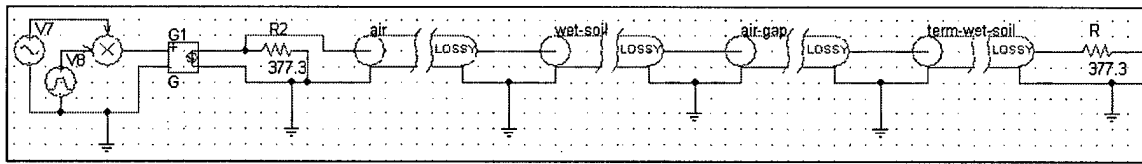


Figure 8(a). Air-wetsoil-air-wetsoil model. With lengths as air = 3m, wetsoil = 0.1m, airgap = 1cm and wetsoil = 10m.

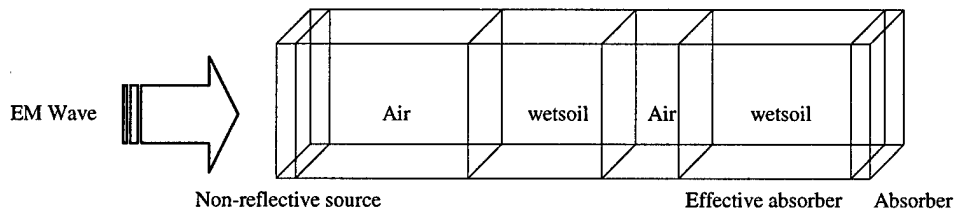


Figure 8(b): Analogy of circuit in Fig. 8(a).

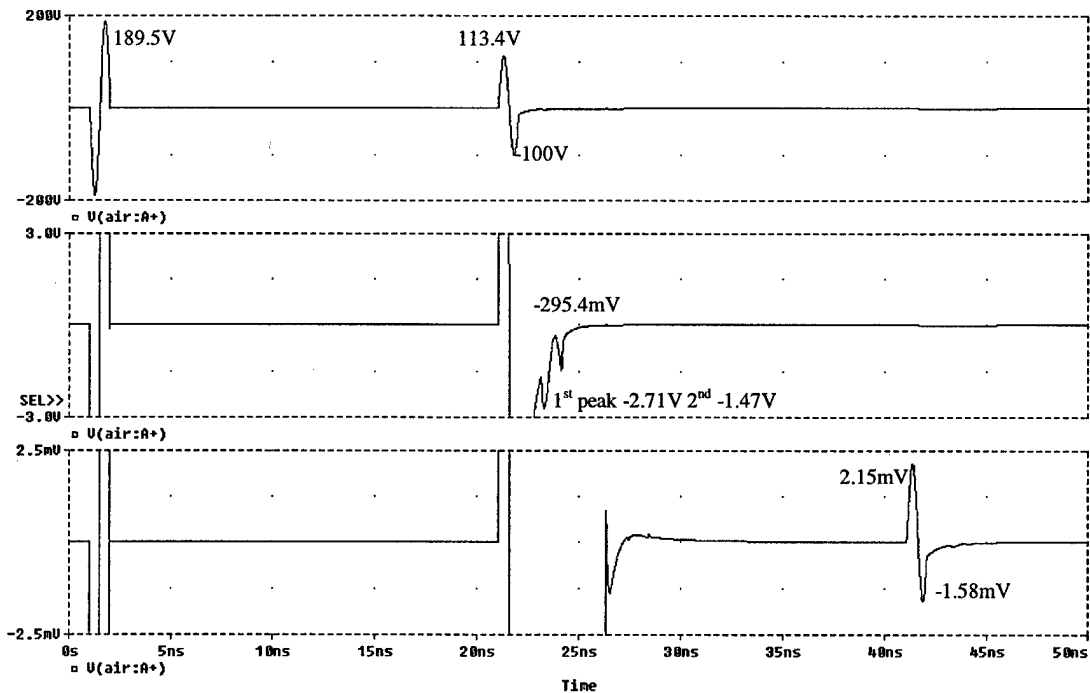


Figure 8(c). Voltage at the antenna (R5 in Fig. 8(a)) for Air-wetsoil-air-wetsoil model, With lengths as air = 3m, wetsoil = 0.1m, airgap = 1cm and wetsoil = 10m. Top: Normal view. First reflection occurs at 21ns. Bottom: Magnified view.

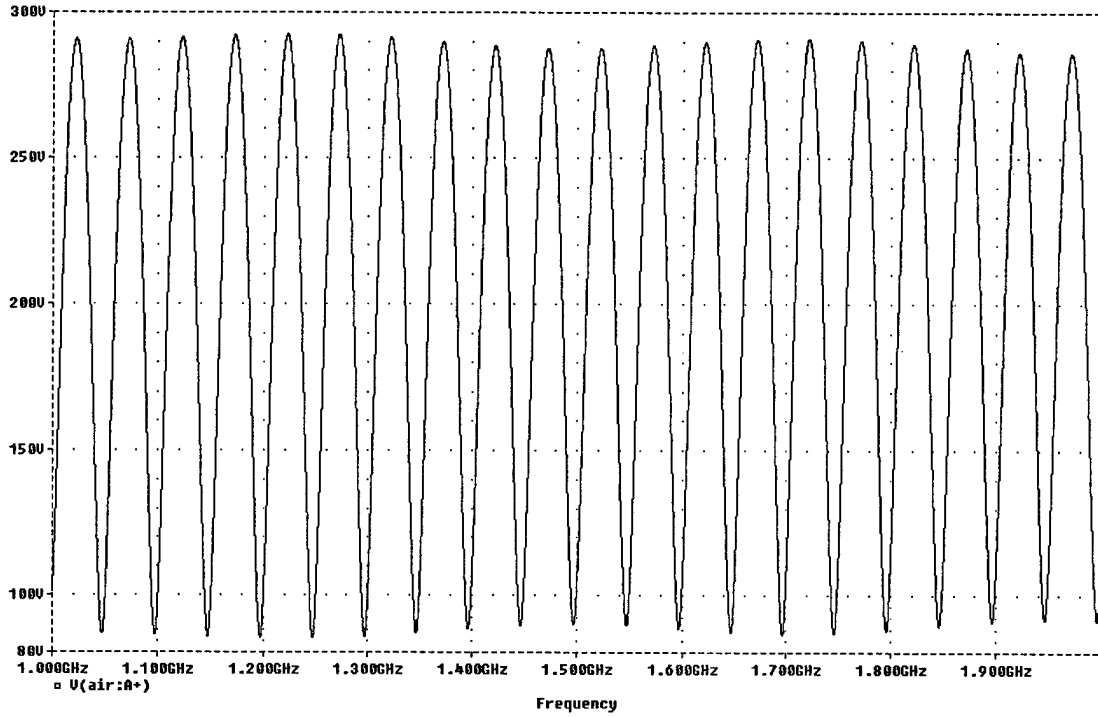


Figure 8(d). Voltage at the antenna (R5 in Fig. 8(a)) for Air-wetsoil-air-wetsoil model, With lengths as air = 3m, wetsoil = 0.1m, airgap = 1cm and wetsoil = 10m. Frequency Sweep plot from 1GHz to 2GHz

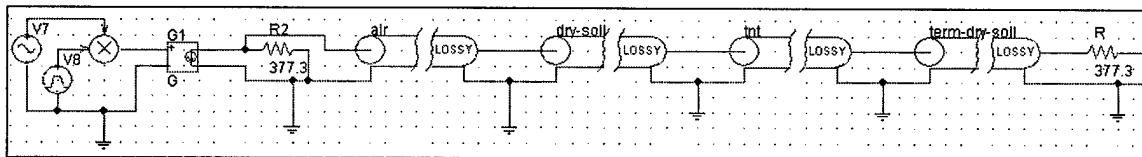


Figure 9(a): Air-drysoil-TNT-drysoil model. With lengths as air = 3m, drysoil = 0.25m, TNT = 10cm and drysoil = 100m.

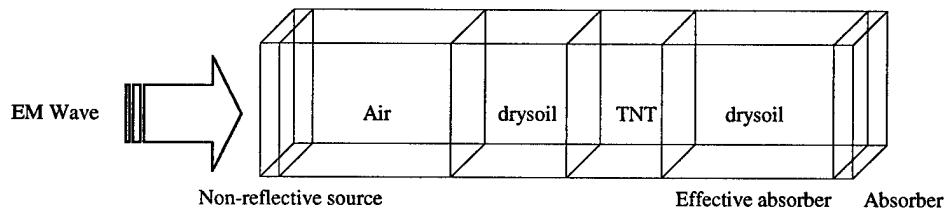


Figure 9(b): Analogy of circuit in Fig. 9(a).

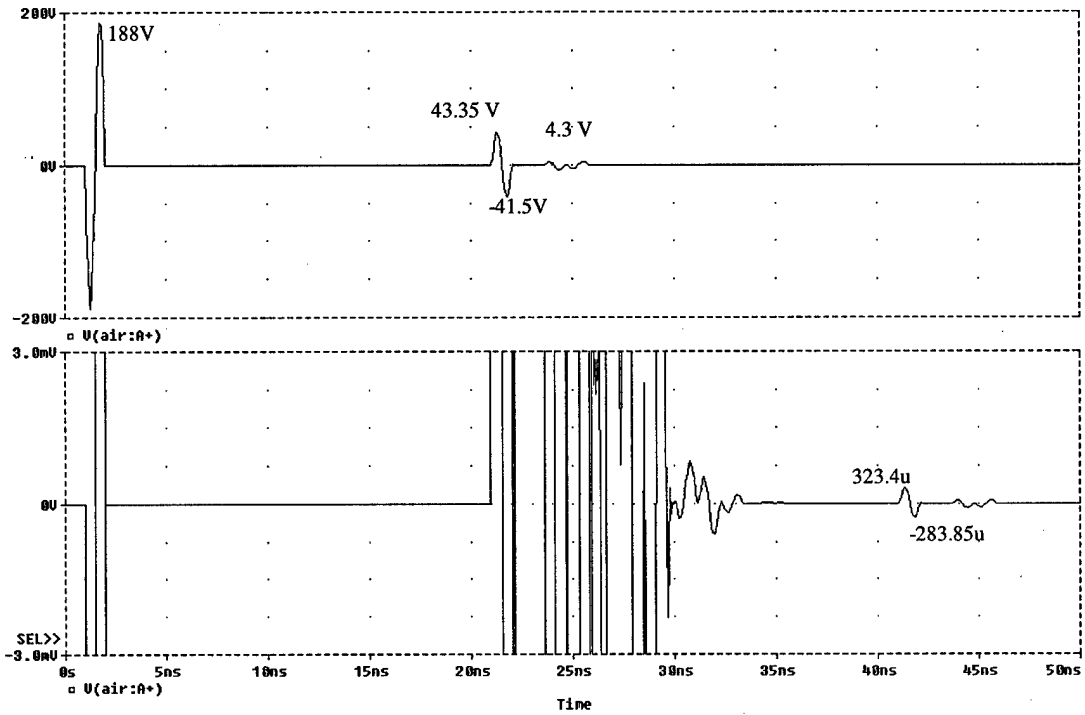


Figure 9(c). Voltage at the antenna (R5 in Fig. 9(a)) for Air-drysoil-TNT-drysoil model, with lengths as air = 3m, drysoil = 0.25m, TNT = 10cm and drysoil = 100m. Top: Normal view. First reflection occurs at 21ns. Bottom: Magnified view.

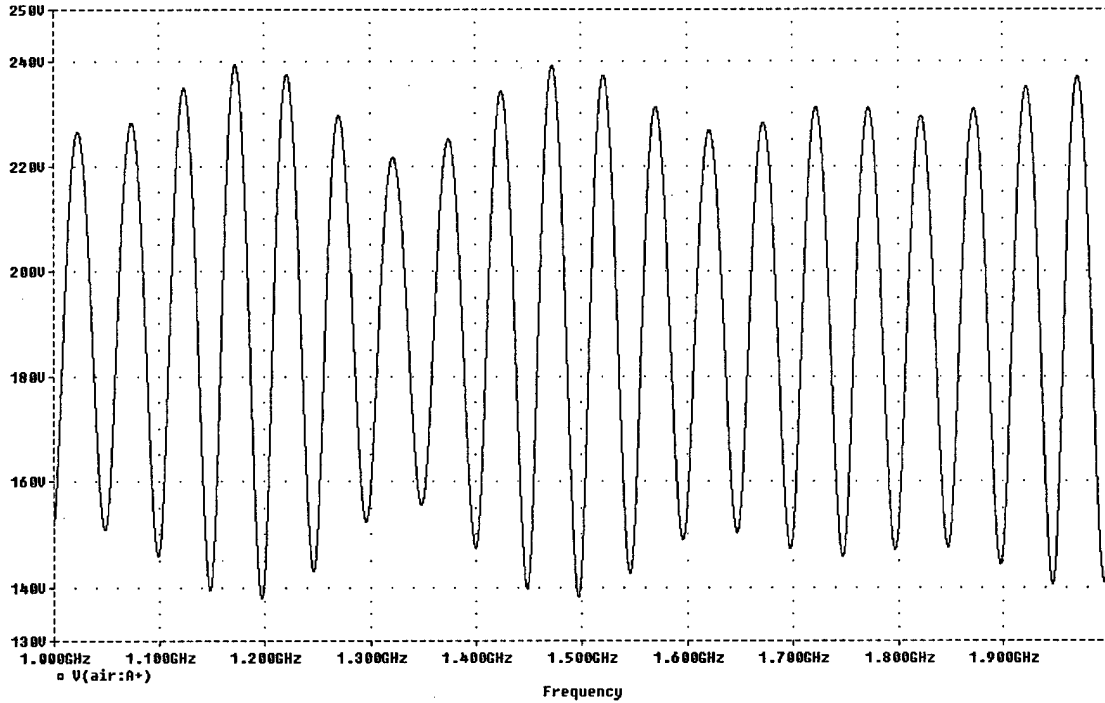


Figure 9(d). Voltage at the antenna (R5 in Fig. 9(a)) for Air-drysoil-TNT-drysoil model, with lengths as air = 3m, drysoil = 0.25m, TNT = 10cm and drysoil = 100m. Frequency Sweep plot from 1GHz to 2GHz

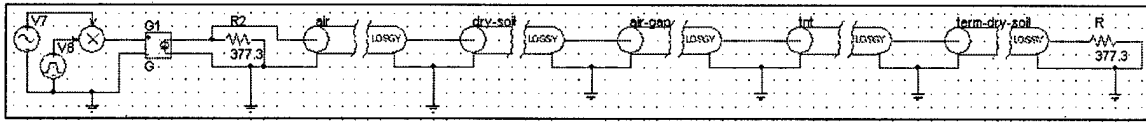


Figure 10(a): Air-drysoil-airgap-TNT-drysoil model. With lengths as air = 3m, drysoil = 0.25m, airgap = 1cm, TNT = 9cm, and drysoil = 100m.

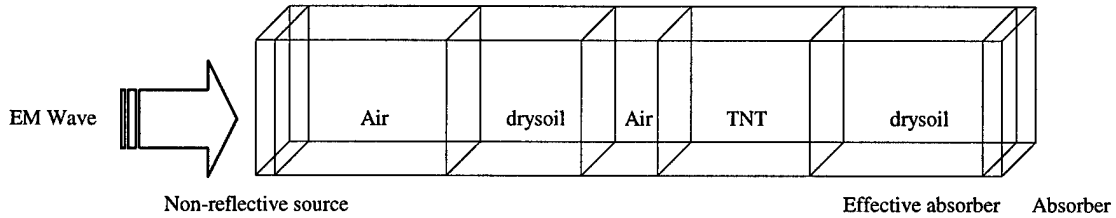


Figure 10(b): Analogy of circuit in Fig 10(a).

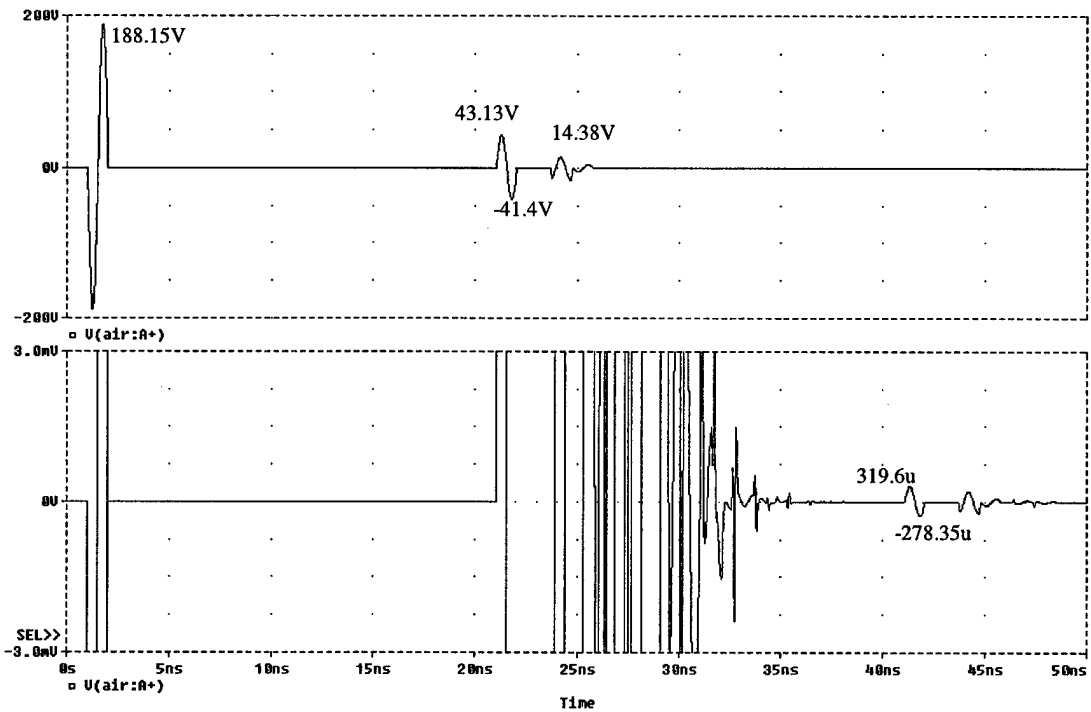


Figure 10(c). Voltage at the antenna (R5 in Fig. 10(a)) for Air-drysoil-airgap-TNT-drysoil model, with lengths as air = 3m, drysoil = 0.25m, airgap = 1cm, TNT = 9cm and drysoil = 100m. Top: Normal view. First reflection occurs at 21ns. Bottom: Magnified view.

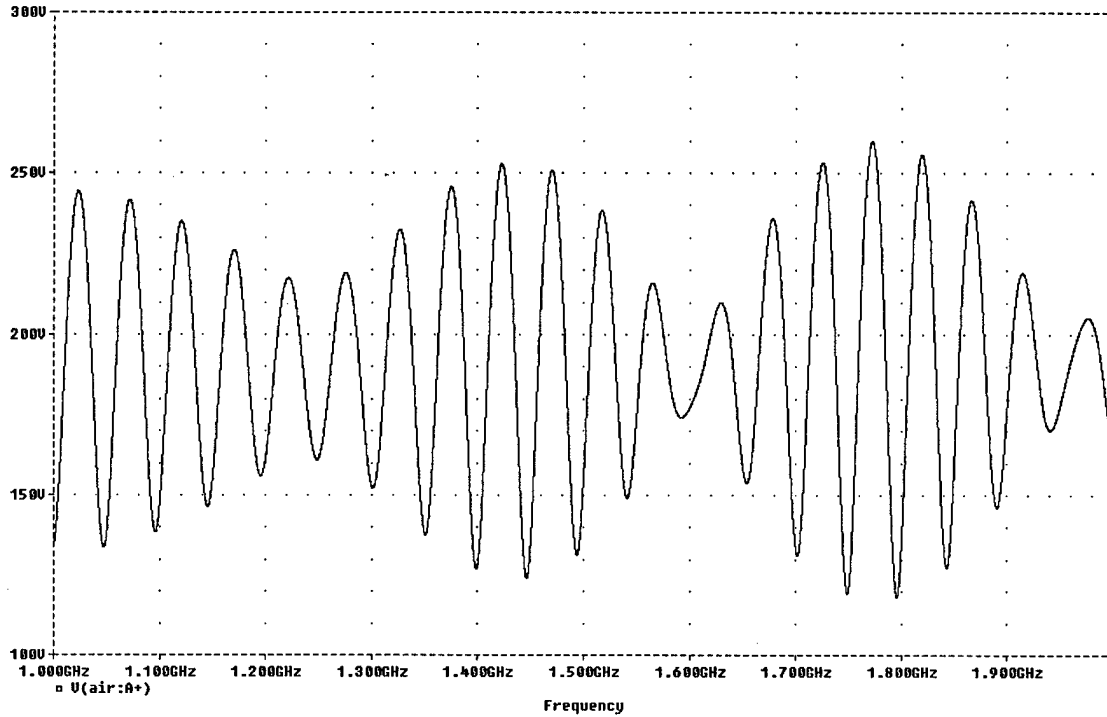


Figure 10(d). Voltage at the antenna (R5 in Fig. 10(a)) for Air-drysoil-airgap-TNT-drysoil model, with lengths as air = 3m, drysoil = 0.25m, airgap = 1cm, TNT = 9cm and drysoil = 100m. Frequency Sweep plot from 1GHz to 2GHz

4. Comparisons

Table 2: Comparison between measured and predicted loss.

	Predicted loss	Measured loss	Published Data [3]
Dry soil	3.62 dB/m	3.74 dB/m	2 dB/m
Wet soil 13% moisture	141 dB/m	130 dB/m	100 dB/m

Table 3: Amplitude of Voltage wave.

Model	V amplitude at Antenna	V amplitude of reflection from ground	V amplitude of reflection from target/ground
Air-drysoil-air-drysoil	188.56 V	43.13 V	12.5 V
Air-wetsoil-air-wetsoil	189.5 V	113.4 V	-295.4mV
Air-drysoil-TNT-drysoil	188 V	43.35 V	4.3 V
Air-drysoil-airgap-TNT-drysoil	188.15 V	43.13 V	14.38 V

5. Conclusions

The experiments with air gap and TNT for the mine are representative of targets in the field. This situation was depicted in the experiments of Fig. 10 and is the focus of our research. We will focus on this case for developing mathematical models in dry and wet soil.

6. References

1. Hayt, William H., "Engineering Electromagnetics".
2. Anh H. Trang, "Simulation of Mine detection over Dry soil, Snow, Ice and Water", SPIE Vol. 2765.
3. US Army Data, Belvoir RD&E Center.

7. Attribution

This material is based upon work supported by the U.S. Army Research Office under contract number DAAG55-98-1-0401.